Guided Formation Control for Wheeled Mobile Robots

Morten Breivik†, Maxim V. Subbotin‡, and Thor I. Fossen†

Abstract— **This paper considers the topic of formation control for wheeled mobile robots (WMRs). Specifically, the work deals with unicycle-type WMRs (i.e., underactuated vehicles that experience a lateral zero-speed constraint, such that their linear velocity at all times is aligned with the longitudinal axis of symmetry). Within a leader-follower framework, a so-called guided formation control scheme is developed by means of a modular design procedure which is inspired by concepts from integrator backstepping and cascade theory. Control, guidance, and synchronization laws ensure that each individual formation member is able to converge to and maintain its assigned formation position such that the overall formation is able to assemble and maintain itself while traversing a regularly parameterized path that is chosen by a formation control designer. The proposed version of the guided approach is completely decentralized in the sense that no variables need to be communicated between the formation members (hence, the formation suffers from graceful degradation). A key quality of the suggested scheme is helmsman-like transient motion behavior, which is illustrated through a computer simulation involving three unicycle-type WMRs.**

I. Introduction

Formation control technology is playing an increasingly important role for commercial, scientific, and military purposes. Today, relevant applications can be found everywhere; at sea, on land, in the air, and in space. The ongoing development is enabled by progress within sensor, communication, and computer technology, and has a main focus toward fully autonomous operations. Particularly, self-reliant and self-contained vehicle formations are desirable for solving important tasks in so-called dirty, dull, and dangerous environments. The vehicles can act as scouts, nodes in communication and sensor networks, or elements within battlegroups. There is generally strength in numbers, and multi-vehicle operations render possible tasks that no single vehicle can solve, as well as increase operational robustness toward individual failures. Specifically, this paper deals with underactuated land-based operations by considering formation control for wheeled mobile robots (WMRs) of the unicycle type.

This work was supported by the Research Council of Norway through the Centre for Ships and Ocean Structures at the Norwegian University of Science and Technology.

† {Centre for Ships and Ocean Structures, Department of Engineering Cybernetics}, Norwegian University of Science and Technology, NO-7491 Trondheim, Norway; {morten.breivik, fossen}@ieee.org.

‡Department of Electrical and Computer Engineering, University of California, Santa Barbara, CA 93106, USA; subbotin@engineering.ucsb.edu

A. Previous Work

Research within formation control theory can be divided into two main categories; the analytical and the algorithmic. The analytical category represents those approaches that are most readily analyzed by mathematical tools, and include both leader-follower methods and virtual structure methods. On the other hand, the algorithmic category represents those approaches that are not readily analyzed mathematically, but have to be numerically simulated by means of a computer in order to investigate their (emergent) behavior. So-called behavior-based methods belong to this last category.

Previous work in the leader-follower vein can be found in [1], where graph theory and nonlinear control theory are used to investigate transitions between different formation structures; in [2], which considers structural formation stabilization by means of nonlinear MPC theory; in [3], where omnidirectional visual servoing is used for formation control purposes; in [4], which proposes a decentralized scheme to minimize inter-vehicle communication; and in [5], where nonlinear cascade and synchronization theory is used to achieve formation tracking.

Work within the virtual structure framework is proposed in [6], where the concept is initially introduced (as a scheme where each formation member is regarded equivalent to a particle embedded in a rigid geometric structure); in [7], where a so-called formation function is proposed as a measure of formation maintenance; and in [8], where the formation control problem is decoupled into a planning problem and a tracking problem.

Behavioral methods are reported in [9], which investigates fundamental properties related to behavior-based design; in [10], where four different formation patterns and three different formation reference definitions are investigated by means of so-called motor schemas through computer simulations, laboratory experiments, and outdoor experiments; in [11], where a number of cooperative behaviors are examined by employing so-called social potential fields; in [12], which explores formation transition strategies illustrated by laboratory experiments; and in [13], where a hierarchical formation control methodology is proposed and experimentally tested.

Finally, the anthologies [14] and [15] report state-of-the-art concepts for group coordination and cooperative control, while the book [16] considers a multitude of interesting and relevant robotic systems as well as their applications.

B. Main Contribution

The main contribution of this paper is a concept named *guided formation control*. Developed within a leader-follower framework, the scheme is based on principles from integrator backstepping design [17] as well as theory for nonlinear time-varying cascades [18]. The proposed design procedure for each individual WMR is completely modular, and consists of three distinct steps where control, guidance, and synchronization laws are sequentially derived. The approach represents an entirely decentralized scheme (suffering from graceful degradation), where each formation member displays helmsman-like motion behavior during the transient formation assembly phase. All regularly parameterized paths are rendered feasible by the suggested concept.

II. Guided Formation Control

This section develops the concept of guided formation control for wheeled mobile robots of the unicycle type. In what follows, the time derivative of a vector $\mathbf{x}(t)$ is denoted $\dot{\mathbf{x}}$, the partial derivative of a vector $\mathbf{x}(\varpi(t))$ is denoted $\mathbf{x}'$ $\left(= \frac{\partial \mathbf{x}}{\partial \varpi}(\varpi(t))\right)$, while $|\cdot|$ represents the Euclidean vector norm as well as the induced matrix norm.

A. Dynamic Model of a Wheeled Mobile Robot

Consider a unicycle-type WMR as depicted in Figure 1. The WMR employs two fore-mounted driving wheels (attached along the same axis) as active actuators, with an aft-mounted support wheel that is passive and freely rotating. The interaction between the wheels and the ground is assumed to be purely of a rolling nature, i.e., slipping never occurs. The center of gravity (CG) of the WMR is assumed to be located at the intersection of the lateral front-wheel axis and the longitudinal symmetry axis of the vehicle. Hence, the body-fixed coordinate system is selected to be situated there.

A dynamic model of the considered WMR consists of the kinematics

$$\dot{\boldsymbol{\eta}} = \begin{bmatrix} \cos\theta & 0 \\ \sin\theta & 0 \\ 0 & 1 \end{bmatrix} \boldsymbol{\nu} \tag{1}$$

and the kinetics

$$\mathbf{M}\dot{\boldsymbol{\nu}} = \boldsymbol{\tau}, \tag{2}$$

where $\boldsymbol{\eta} = [x, y, \theta]^\top \in \mathbb{R}^2 \times \mathcal{S}$ represents the inertial position (of the WMR CG) and orientation (with $\mathcal{S} = [-\pi, \pi]$), $\boldsymbol{\nu} = [u, \omega]^\top \in \mathbb{R}^2$ represents the body-fixed velocity,

$$\mathbf{M} = \begin{bmatrix} m & 0 \\ 0 & I \end{bmatrix} \tag{3}$$

represents the inertia matrix (where m and I represent the WMR mass and moment of inertia, respectively), and $\boldsymbol{\tau} \in \mathbb{R}^2$ represents the body-fixed actuator force and moment.

Since the considered type of WMR travels on a surface without slipping, and is unactuated in the lateral direction, it experiences no lateral speed. This inherently gives rise to the nonholonomic constraint equation $\dot{y}\cos\theta - \dot{x}\sin\theta = 0$, which means that the linear velocity of the WMR is aligned with the WMR orientation (i.e., along the longitudinal symmetry axis of the WMR). Hence, the orientation of the WMR must be actively employed to direct its linear velocity. This is for instance not the case for a fully actuated vehicle, where the direction of the linear velocity is independent of the vehicle orientation since all the degrees of freedom are independently actuated (at the same time).

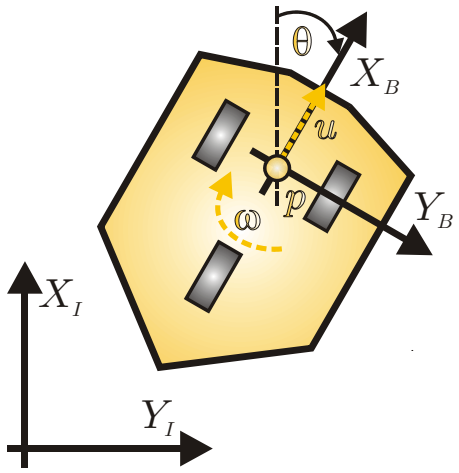

Fig. 1. The unicycle-type WMR under consideration; employing two fore-mounted driving wheels and an aft-mounted freely rotating support wheel.

B. Formation Control Scenario

This paper considers formation control within a leader-follower framework, where a formation structure is defined relative to a virtual formation leader. It is assumed that the formation control designer can choose both the path to be traversed by the leader, the temporal motion of the leader, as well as the geometric formation structure defined relative to the leader. Consequently, consider a planar path continuously parameterized by a scalar variable $\varpi \in \mathbb{R}$, such that the position of a point belonging to the path is represented by $\mathbf{p}_\mathrm{p}(\varpi) \in \mathbb{R}^2$. Thus, the path is a one-dimensional manifold that can be expressed by the set

$$\mathcal{P} = \left\{ \mathbf{p} \in \mathbb{R}^2 \mid \mathbf{p} = \mathbf{p}_\mathrm{p}(\varpi) \ \forall \varpi \in \mathbb{R} \right\}. \tag{4}$$

Then, represent the virtual formation leader by $\mathbf{p}_\mathrm{l}(t) = \mathbf{p}_\mathrm{p}(\varpi_\mathrm{l}(t))$. The leader traverses the path by adhering to a speed profile $U_\mathrm{l}(\varpi_\mathrm{l}, t)$, implemented through

$$\dot{\varpi}_\mathrm{l} = \frac{U_\mathrm{l}(\varpi_\mathrm{l}, t)}{\left|\mathbf{p}'_\mathrm{p}(\varpi_\mathrm{l})\right|}, \tag{5}$$

since $|\dot{\mathbf{p}}_\mathrm{l}| = \left|\mathbf{p}'_\mathrm{p}(\varpi_\mathrm{l})\right| \dot{\varpi}_\mathrm{l} = U_\mathrm{l}$, where $U_\mathrm{l} \in [U_{\mathrm{l,min}}, U_{\mathrm{l,max}}]$, $U_{\mathrm{l,min}} > 0$ (non-negative by definition).

Furthermore, consider a formation consisting of n members, each uniquely identified through the index set $\mathcal{I} = \{1, ..., n\}$. The assigned formation position for member i is represented by $\mathbf{p}_{\mathrm{f,i}}(t)$, which is related to the formation leader through a chosen geometric assignment (defined in local, path-tangential

coordinates relative to the leader). By design, we ensure that no formation positions are identical, i.e., $\mathbf{p}_{\mathrm{f,i}} \neq \mathbf{p}_{\mathrm{f,j}}\ \forall i \neq j$, where $i, j \in \mathcal{I}$.

1) Problem Statement: The formation control problem for the type of WMRs under consideration can be stated by

$$\lim_{t\to\infty} \left(\boldsymbol{\eta}_{\mathrm{i}}(t) - \boldsymbol{\eta}_{\mathrm{f,i}}(t)\right) = \mathbf{0}\ \forall i \in \mathcal{I}, \tag{6}$$

where $\boldsymbol{\eta}_{\mathrm{i}}(t)$ represents the ith formation member, and $\boldsymbol{\eta}_{\mathrm{f,i}}(t) = \left[\mathbf{p}_{\mathrm{f,i}}^{\top}(t), \theta_{\mathrm{f,i}}(t)\right]^{\top} \in \mathbb{R}^2 \times \mathcal{S}$, where $\theta_{\mathrm{f,i}}(t)$ is the path-tangential orientation at $\mathbf{p}_{\mathrm{l}}(t)$. Note that the asymptotic nature of this problem statement does not dictate the desired transient orientation $\theta_{\mathrm{d,i}}(t)$ required to converge to $\mathbf{p}_{\mathrm{f,i}}(t)$. Also note that if the WMRs had been fully actuated, then $\theta_{\mathrm{f,i}}(t)$ could have been chosen arbitrarily, e.g., to satisfy some auxiliary task objective. See Figure 2 for an illustration of the formation control concept under consideration.

C. Motion Control of Individual Formation Members

This section develops the control, guidance and synchronization laws that each formation member must employ in order to converge to its assigned position in the formation. The underlying motion control concept is adapted from [19], and entails a three-step, backstepping-inspired, and cascaded-based modular design procedure.

1) Step 1: Control Loop Design: Since the position of a vehicle can be controlled through its linear velocity, we redefine the control output space from the nominal 3 DOF position and heading to the 2 DOF (longitudinal) speed and orientation (these two variables comprise the linear velocity in our case). Thus, the vehicle is no longer underactuated in the control output space, but nevertheless unavoidably suffers from the nonholonomic constraint on the lateral speed.

Consequently, consider the positive definite and radially unbounded Control Lyapunov Function (CLF)

$$V_{\mathrm{g}} = \frac{1}{2}(z_\theta^2 + \mathbf{z}_\nu^{\top}\mathbf{M}\mathbf{z}_\nu) \tag{7}$$

where we have

$$z_\theta = \theta - \theta_{\mathrm{d}} \tag{8}$$

and

$$\mathbf{z}_\nu = \boldsymbol{\nu} - \boldsymbol{\alpha}, \tag{9}$$

where $\boldsymbol{\alpha} = [\alpha_{\mathrm{u}}, \alpha_\omega]^{\top} \in \mathbb{R}^2$ is a vector of stabilizing functions yet to be designed (virtual inputs that become reference signals). Subsequently, differentiate the CLF with respect to time to obtain

$$\begin{aligned} \dot{V}_{\mathrm{g}} &= z_\theta \dot{z}_\theta + \mathbf{z}_\nu^{\top}\mathbf{M}\dot{\mathbf{z}}_\nu \\ &= z_\theta(\dot{\theta} - \dot{\theta}_{\mathrm{d}}) + \mathbf{z}_\nu^{\top}\mathbf{M}(\dot{\boldsymbol{\nu}} - \dot{\boldsymbol{\alpha}}) \\ &= z_\theta(\mathbf{h}^{\top}\boldsymbol{\nu} - \omega_{\mathrm{d}}) + \mathbf{z}_\nu^{\top}(\mathbf{M}\dot{\boldsymbol{\nu}} - \mathbf{M}\dot{\boldsymbol{\alpha}}) \end{aligned}$$

where

$$\mathbf{h} = [0, 1]^{\top}. \tag{10}$$

Furthermore, by employing $\boldsymbol{\nu} = \mathbf{z}_\nu + \boldsymbol{\alpha}$, we obtain

$$\dot{V}_{\mathrm{g}} = z_\theta(\mathbf{h}^{\top}\boldsymbol{\alpha} - \omega_{\mathrm{d}}) + \mathbf{z}_\nu^{\top}(\boldsymbol{\tau} - \mathbf{M}\dot{\boldsymbol{\alpha}} + \mathbf{h}z_\theta),$$

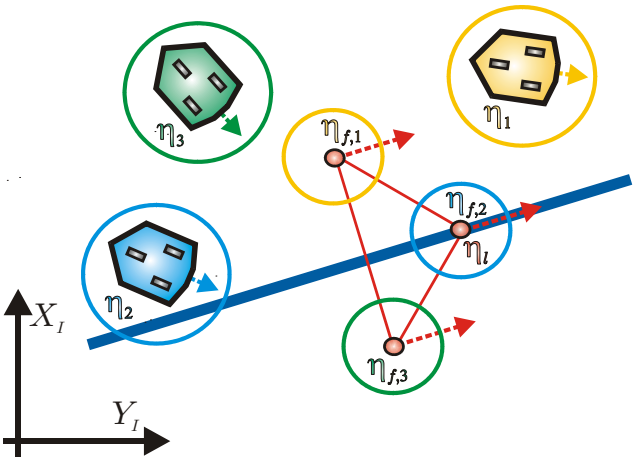

Fig. 2. The formation members attempt to assemble and maintain the geometric structure defined relative to the path-traversing virtual leader.

which results in the quadratically negative definite

$$\dot{V}_{\mathrm{g}} = -k_\theta z_\theta^2 - \mathbf{z}_\nu^{\top}\mathbf{K}_\nu\mathbf{z}_\nu \tag{11}$$

when choosing the virtual input $\mathbf{h}^{\top}\boldsymbol{\alpha} = \alpha_\omega$ as

$$\alpha_\omega = \omega_{\mathrm{d}} - k_\theta z_\theta, \tag{12}$$

where $k_\theta > 0$ is a constant, and by selecting the control input as

$$\boldsymbol{\tau} = \mathbf{M}\dot{\boldsymbol{\alpha}} - \mathbf{h}z_\theta - \mathbf{K}_\nu\mathbf{z}_\nu, \tag{13}$$

where $\mathbf{K}_\nu = \mathbf{K}_\nu^{\top} > 0$ is a constant matrix.

Considering the state vector $\mathbf{z}_{\mathrm{g}} = \left[z_\theta, \mathbf{z}_\nu^{\top}\right]^{\top}$, the following proposition can now be stated

Proposition 1: The equilibrium point $\mathbf{z}_{\mathrm{g}} = \mathbf{0}$ is rendered uniformly globally exponentially stable (UGES) by adhering to (12) and (13) under the assumption that $\boldsymbol{\alpha}$ and $\dot{\boldsymbol{\alpha}}$ are uniformly bounded.

Proof: By standard Lyapunov theory, (7) and (11) show that the origin of $\mathbf{z}_{\mathrm{g}}$ is UGES. ■

Note that this heading and velocity controller cannot achieve anything meaningful unless it is fed sensible reference signals, i.e., unless θ_{d} and α_{u} are purposefully defined. This task is the responsibility of the final two design steps.

2) Step 2: Guidance Loop Design: We now design the required *orientation* of the WMR linear velocity (in our case equivalent to θ_{d}) such that a wheeled mobile robot controlled by (13) applying (12) attains its assigned formation position relative to the path (even though it may not be synchronized with the leader).

Consequently, consider the positive definite and radially unbounded CLF

$$V_{\tilde{\varepsilon}} = \frac{1}{2}\tilde{\boldsymbol{\varepsilon}}^{\top}\tilde{\boldsymbol{\varepsilon}}, \tag{14}$$

with

$$\tilde{\boldsymbol{\varepsilon}} = \boldsymbol{\varepsilon} - \boldsymbol{\varepsilon}_{\mathrm{f}} \tag{15}$$

and

$$\boldsymbol{\varepsilon} = \mathbf{R}_{\mathrm{C}}^{\top}(\mathbf{p} - \mathbf{p}_{\mathrm{c}}), \tag{16}$$

where $\mathbf{p}_\mathrm{c} = \mathbf{p}_\mathrm{p}(\varpi_\mathrm{c})$ represents a (virtual) *collaborator* point that acts cooperatively with the WMR as an intermediate path attractor, such that the vehicle can converge to its assigned formation position relative to the path (i.e., ε_f) irrespective of whether it has synchronized with the formation leader or not. Furthermore, the path-tangential reference frame at $\mathbf{p}_\mathrm{c}$ is termed the COLLABORATOR frame (**C**). To arrive at **C**, the INERTIAL frame (**I**) must be positively rotated an angle

$$\chi_\mathrm{c} = \arctan\left(\frac{y'_\mathrm{p}(\varpi_\mathrm{c})}{x'_\mathrm{p}(\varpi_\mathrm{c})}\right), \tag{17}$$

which can be represented by the rotation matrix

$$\mathbf{R}_\mathrm{C} = \begin{bmatrix} \cos\chi_\mathrm{c} & -\sin\chi_\mathrm{c} \\ \sin\chi_\mathrm{c} & \cos\chi_\mathrm{c} \end{bmatrix}, \tag{18}$$

$\mathbf{R}_\mathrm{C} \in SO(2)$. Hence, equation (16) represents the error vector between the WMR and its collaborator decomposed in **C**. The local coordinates $\boldsymbol{\varepsilon} = [s, e]^\top$ consist of the *along-track error* s and the *cross-track error* e. By driving $\tilde{\boldsymbol{\varepsilon}}$ to zero, $\boldsymbol{\varepsilon}$ becomes equal to $\boldsymbol{\varepsilon}_\mathrm{f}$ such that the WMR attains its assigned path-relative formation position. It is assumed that $\boldsymbol{\varepsilon}_\mathrm{f}$, $\dot{\boldsymbol{\varepsilon}}_\mathrm{f}$ and $\ddot{\boldsymbol{\varepsilon}}_\mathrm{f}$ are uniformly bounded, and nominally $\dot{\boldsymbol{\varepsilon}}_\mathrm{f} = \ddot{\boldsymbol{\varepsilon}}_\mathrm{f} = \mathbf{0}$.

Now, differentiate the CLF in (14) along the trajectories of $\tilde{\boldsymbol{\varepsilon}}$ to obtain

$$\begin{aligned} \dot{V}_{\tilde{\varepsilon}} &= \tilde{\boldsymbol{\varepsilon}}^\top \dot{\tilde{\boldsymbol{\varepsilon}}} \\ &= \tilde{\boldsymbol{\varepsilon}}^\top (\mathbf{S}_\mathrm{C}^\top \mathbf{R}_\mathrm{C}^\top (\mathbf{p} - \mathbf{p}_\mathrm{c}) + \mathbf{R}_\mathrm{C}^\top (\dot{\mathbf{p}} - \dot{\mathbf{p}}_\mathrm{c}) - \dot{\boldsymbol{\varepsilon}}_\mathrm{f}) \\ &= \tilde{\boldsymbol{\varepsilon}}^\top \left(\mathbf{S}_\mathrm{C}^\top \boldsymbol{\varepsilon} + \mathbf{R}_\mathrm{C}^\top \mathbf{v}^\mathrm{I} - \mathbf{v}_\mathrm{c}^\mathrm{C} - \dot{\boldsymbol{\varepsilon}}_\mathrm{f}\right) \\ &= \tilde{\boldsymbol{\varepsilon}}^\top \left(\mathbf{S}_\mathrm{C}^\top \tilde{\boldsymbol{\varepsilon}} + \mathbf{S}_\mathrm{C}^\top \boldsymbol{\varepsilon}_\mathrm{f} + \mathbf{R}_\mathrm{C}^\top \mathbf{v}^\mathrm{I} - \mathbf{v}_\mathrm{c}^\mathrm{C} - \dot{\boldsymbol{\varepsilon}}_\mathrm{f}\right) \\ &= \tilde{\boldsymbol{\varepsilon}}^\top \left(\mathbf{R}_\mathrm{C}^\top \mathbf{v}^\mathrm{I} - \mathbf{v}_\mathrm{c}^\mathrm{C} + \mathbf{S}_\mathrm{C}^\top \boldsymbol{\varepsilon}_\mathrm{f} - \dot{\boldsymbol{\varepsilon}}_\mathrm{f}\right), \end{aligned}$$

where $\dot{\mathbf{R}}_\mathrm{C} = \mathbf{R}_\mathrm{C}\mathbf{S}_\mathrm{C}$ with $\mathbf{S}_\mathrm{C} = -\mathbf{S}_\mathrm{C}^\top \Rightarrow \tilde{\boldsymbol{\varepsilon}}^\top \mathbf{S}_\mathrm{C}^\top \tilde{\boldsymbol{\varepsilon}} = 0$, $\dot{\mathbf{p}} = \mathbf{v}^\mathrm{I}$ represents the linear velocity of the WMR decomposed in **I**, and $\mathbf{v}_\mathrm{c}^\mathrm{C} = [U_\mathrm{c}, 0]^\top$ ($U_\mathrm{c} = |\dot{\mathbf{p}}_\mathrm{c}|$) represents the linear velocity of the collaborator decomposed in **C**. Furthermore,

$$\begin{aligned} \dot{V}_{\tilde{\varepsilon}} &= \tilde{\boldsymbol{\varepsilon}}^\top \left(\mathbf{R}_\mathrm{C}^\top \boldsymbol{\alpha}_\mathrm{v}^\mathrm{I} - \mathbf{v}_\mathrm{c}^\mathrm{C} + \mathbf{S}_\mathrm{C}^\top \boldsymbol{\varepsilon}_\mathrm{f} - \dot{\boldsymbol{\varepsilon}}_\mathrm{f}\right) + \\ &\quad \tilde{\boldsymbol{\varepsilon}}^\top \mathbf{R}_\mathrm{C}^\top \mathbf{z}_\mathrm{v}^\mathrm{I} \end{aligned} \tag{19}$$

when we employ $\mathbf{z}_\mathrm{v}^\mathrm{I} = \mathbf{v}^\mathrm{I} - \boldsymbol{\alpha}_\mathrm{v}^\mathrm{I}$, where $\boldsymbol{\alpha}_\mathrm{v}^\mathrm{I}$ represents the desired (i.e., ideal) linear velocity of the WMR decomposed in **I**.

We now introduce a (virtual) *mediator* point located at $\mathbf{p}_\mathrm{m}$, which is defined such that when the WMR converges to its assigned formation position relative to the path, the mediator converges to the path. Hence, $\boldsymbol{\varepsilon}_\mathrm{m} = \tilde{\boldsymbol{\varepsilon}}$, and the relationship between the WMR, the mediator, and the collaborator can be expressed by (see Figure 3 for an illustration)

$$\begin{aligned} \boldsymbol{\varepsilon} &= \boldsymbol{\varepsilon}_\mathrm{m} + \boldsymbol{\varepsilon}_\mathrm{f} && (20) \\ &= \mathbf{R}_\mathrm{C}^\top (\mathbf{p}_\mathrm{m} - \mathbf{p}_\mathrm{c}) + \boldsymbol{\varepsilon}_\mathrm{f} && (21) \\ &= \mathbf{R}_\mathrm{C}^\top (\mathbf{p} - \mathbf{p}_\mathrm{c}) && (22) \end{aligned}$$

such that

$$\mathbf{p}_\mathrm{m} = \mathbf{p} - \mathbf{R}_\mathrm{C}\boldsymbol{\varepsilon}_\mathrm{f}, \tag{23}$$

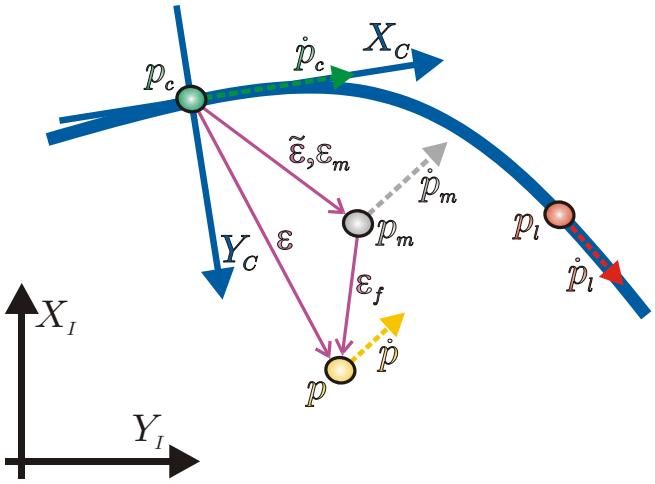

Fig. 3. The fundamental geometry underlying the principle of guided formation control. The WMR is located at $\mathbf{p}$ (orange), the mediator at $\mathbf{p}_\mathrm{m}$ (grey), the collaborator at $\mathbf{p}_\mathrm{c}$ (green), and the virtual leader at $\mathbf{p}_\mathrm{l}$ (red).

which is used to compute (and continuously update) the location of the mediator.

Hence,

$$\dot{\mathbf{p}}_\mathrm{m} = \dot{\mathbf{p}} - \dot{\mathbf{R}}_\mathrm{C}\boldsymbol{\varepsilon}_\mathrm{f} - \mathbf{R}_\mathrm{C}\dot{\boldsymbol{\varepsilon}}_\mathrm{f},$$

which is equal to

$$\mathbf{v}_\mathrm{m}^\mathrm{I} = \mathbf{v}^\mathrm{I} - \mathbf{R}_\mathrm{C}\mathbf{S}_\mathrm{C}\boldsymbol{\varepsilon}_\mathrm{f} - \mathbf{R}_\mathrm{C}\dot{\boldsymbol{\varepsilon}}_\mathrm{f}, \tag{24}$$

entailing that

$$\boldsymbol{\alpha}_{\mathrm{v,m}}^\mathrm{I} = \boldsymbol{\alpha}_\mathrm{v}^\mathrm{I} - \mathbf{R}_\mathrm{C}\mathbf{S}_\mathrm{C}\boldsymbol{\varepsilon}_\mathrm{f} - \mathbf{R}_\mathrm{C}\dot{\boldsymbol{\varepsilon}}_\mathrm{f}, \tag{25}$$

or rather, that

$$\boldsymbol{\alpha}_\mathrm{v}^\mathrm{I} = \boldsymbol{\alpha}_{\mathrm{v,m}}^\mathrm{I} + \mathbf{R}_\mathrm{C}(\mathbf{S}_\mathrm{C}\boldsymbol{\varepsilon}_\mathrm{f} + \dot{\boldsymbol{\varepsilon}}_\mathrm{f}), \tag{26}$$

which we duly insert into (19) to achieve

$$\dot{V}_{\tilde{\varepsilon}} = \tilde{\boldsymbol{\varepsilon}}^\top \left(\mathbf{R}_\mathrm{C}^\top \boldsymbol{\alpha}_{\mathrm{v,m}}^\mathrm{I} - \mathbf{v}_\mathrm{c}^\mathrm{C}\right) + \tilde{\boldsymbol{\varepsilon}}^\top \mathbf{R}_\mathrm{C}^\top \mathbf{z}_\mathrm{v}^\mathrm{I} \tag{27}$$

since $\mathbf{S}_\mathrm{C} = -\mathbf{S}_\mathrm{C}^\top$. We note that $\boldsymbol{\alpha}_{\mathrm{v,m}}^\mathrm{I}$ represents the desired linear velocity of the mediator (that corresponds to the desired linear velocity of the WMR) decomposed in **I**.

Subsequently, define $\boldsymbol{\alpha}_{\mathrm{v,m}}^\mathrm{I} = \mathbf{R}_\mathrm{DV}\boldsymbol{\alpha}_{\mathrm{v,m}}^\mathrm{DV}$, where $\boldsymbol{\alpha}_{\mathrm{v,m}}^\mathrm{DV} = [U_\mathrm{d,m}, 0]^\top$ ($U_\mathrm{d,m} = |\boldsymbol{\alpha}_{\mathrm{v,m}}^\mathrm{I}|$) represents the desired linear velocity of the mediator decomposed in a DESIRED VELOCITY frame (**DV**), i.e., decomposed along the desired velocity itself. Thus,

$$\begin{aligned} \dot{V}_{\tilde{\varepsilon}} &= \tilde{\boldsymbol{\varepsilon}}^\top \left(\mathbf{R}_\mathrm{C}^\top \mathbf{R}_\mathrm{DV}\boldsymbol{\alpha}_{\mathrm{v,m}}^\mathrm{DV} - \mathbf{v}_\mathrm{c}^\mathrm{C}\right) + \tilde{\boldsymbol{\varepsilon}}^\top \mathbf{R}_\mathrm{C}^\top \mathbf{z}_\mathrm{v}^\mathrm{I} \\ &= \tilde{\boldsymbol{\varepsilon}}^\top \left(\mathbf{R}_\mathrm{R}\boldsymbol{\alpha}_{\mathrm{v,m}}^\mathrm{DV} - \mathbf{v}_\mathrm{c}^\mathrm{C}\right) + \tilde{\boldsymbol{\varepsilon}}^\top \mathbf{R}_\mathrm{C}^\top \mathbf{z}_\mathrm{v}^\mathrm{I} \end{aligned}$$

where $\mathbf{R}_\mathrm{C}^\top(\chi_\mathrm{c})\mathbf{R}_\mathrm{DV}(\chi_\mathrm{d}) = \mathbf{R}_\mathrm{R}(\chi_\mathrm{d} - \chi_\mathrm{c})$ represents the relative orientation between **C** and **DV**. Denote the angular difference by $\chi_\mathrm{r} = \chi_\mathrm{d} - \chi_\mathrm{c}$, and expand the CLF derivative to obtain

$$\dot{V}_{\tilde{\varepsilon}} = \tilde{s}(U_\mathrm{d,m}\cos\chi_\mathrm{r} - U_\mathrm{c}) + \tilde{e}U_\mathrm{d,m}\sin\chi_\mathrm{r} + \tilde{\boldsymbol{\varepsilon}}^\top \mathbf{R}_\mathrm{C}^\top \mathbf{z}_\mathrm{v}^\mathrm{I}.$$

Hence, $U_{\rm c}$ and $\chi_{\rm r}$ can be considered as virtual inputs for driving $\tilde{\boldsymbol{\varepsilon}}$ to zero, given that $U_{\rm d,m} > 0$. Then, choose $U_{\rm c}$ as

$$U_{\rm c} = U_{\rm d,m}\cos\chi_{\rm r} + \gamma\tilde{s} \tag{28}$$

with $\gamma > 0$ constant, and $\chi_{\rm r}$ as the helmsman-like

$$\chi_{\rm r} = \arctan\left(-\frac{\tilde{e}}{\triangle_{\tilde{\rm e}}}\right) \tag{29}$$

with $\triangle_{\tilde{\rm e}} > 0$ (not necessarily constant; a variable that is often referred to as a lookahead distance in literature treating planar path following along straight lines), giving

$$\dot{V}_{\tilde{\varepsilon}} = -\gamma\tilde{s}^2 - U_{\rm d,m}\frac{\tilde{e}^2}{\sqrt{\tilde{e}^2+\triangle_{\tilde{\rm e}}^2}} + \tilde{\boldsymbol{\varepsilon}}^\top\mathbf{R}_{\rm C}^\top\mathbf{z}_{\rm v}^{\rm I}, \tag{30}$$

which means that

$$\dot{\varpi}_{\rm c} = \frac{U_{\rm c}}{|\mathbf{p}_{\rm c}'|} \tag{31}$$

and

$$\chi_{\rm d} = \chi_{\rm c} + \chi_{\rm r}, \tag{32}$$

with $U_{\rm c}$ as in (28), $\chi_{\rm c}$ as in (17), and $\chi_{\rm r}$ as in (29). Equations (31) and (32) indicate that the collaborator continuously leads the mediator (which moves according to the WMR), while the desired linear velocity of the mediator must point toward the path-tangential associated with the collaborator, in the direction of forward motion.

Summing up the guidance loop design so far, we have introduced two virtual participants whose purposes are to guide the WMR toward its assigned path-relative formation position. The use of the collaborator and the mediator ensure that possible kinematic singularities related to the geometry of the consideration (i.e., off-path traversing a curved path) are avoided. They both move according to the WMR, but their locations are used to calculate the desired orientation of the WMR linear velocity required for converging to the specified formation position relative to the path.

Specifically, the desired linear velocity of the WMR is calculated from

$$\boldsymbol{\alpha}_{\rm v}^{\rm I} = \mathbf{R}_{\rm DV}\boldsymbol{\alpha}_{\rm v,m}^{\rm DV} + \mathbf{R}_{\rm C}(\mathbf{S}_{\rm C}\boldsymbol{\varepsilon}_{\rm f} + \dot{\boldsymbol{\varepsilon}}_{\rm f}) \tag{33}$$

since

$$\boldsymbol{\alpha}_{\rm v}^{\rm I} = \mathbf{R}_{\rm DB}\boldsymbol{\alpha}_{\rm v}^{\rm DB}, \tag{34}$$

where $\boldsymbol{\alpha}_{\rm v}^{\rm DB} = [U_{\rm d}, 0]^\top$ ($U_{\rm d} = \alpha_{\rm u} = |\boldsymbol{\alpha}_{\rm v}^{\rm I}|$) represents the desired linear velocity of the WMR decomposed in a DESIRED BODY frame (**DB**), and

$$\mathbf{R}_{\rm DB} = \begin{bmatrix} \cos\theta_{\rm d} & -\sin\theta_{\rm d} \\ \sin\theta_{\rm d} & \cos\theta_{\rm d} \end{bmatrix} \tag{35}$$

represents the associated rotation matrix.

Subsequently, write the system dynamics of $\tilde{\boldsymbol{\varepsilon}}$ and $\mathbf{z}_{\rm v}^{\rm I}$ as

$$\Sigma_1 \quad : \quad \dot{\tilde{\boldsymbol{\varepsilon}}} = \mathbf{f}_1(t,\tilde{\boldsymbol{\varepsilon}}) + \mathbf{g}_1(t)\mathbf{z}_{\rm v}^{\rm I} \tag{36}$$

$$\Sigma_2 \quad : \quad \dot{\mathbf{z}}_{\rm v}^{\rm I} = \mathbf{f}_2(t,\mathbf{z}_{\rm v}^{\rm I}), \tag{37}$$

which is a pure cascade where

$$\mathbf{g}_1(t) = \mathbf{R}_{\rm C}^\top, \tag{38}$$

and where we note that the origin of $\mathbf{z}_{\rm v}^{\rm I}$ is UGES due to the relationship between the dynamics of $\mathbf{z}_{\rm g}$ and $\mathbf{z}_{\rm v}^{\rm I}$.

Then, consider the following assumptions

A.1 $|\mathbf{p}_{\rm p}'| \in \left[|\mathbf{p}_{\rm p}'|_{\rm min}, \infty\right\rangle\ \forall\varpi \in \mathbb{R},\ |\mathbf{p}_{\rm p}'|_{\rm min} > 0$

A.2 $\triangle_{\tilde{\rm e}} \in [\triangle_{\tilde{\rm e},\,\rm min}, \infty\rangle,\ \triangle_{\tilde{\rm e},\,\rm min} > 0$

A.3 $U_{\rm d,m} \in [U_{\rm d,m,min}, \infty\rangle,\ U_{\rm d,m,min} > 0$

Here, assumption A.1 means that the involved geometric path must be regularly parameterized, assumption A.2 implies that the desired moderator motion must be in the path-tangential direction, while assumption A.3 represents a minimum-speed requirement on the desired linear velocity of the mediator.

By contemplating $\boldsymbol{\xi} = \left[\tilde{\boldsymbol{\varepsilon}}^\top, \mathbf{z}_{\rm v}^{\rm I\top}\right]^\top$, we arrive at

Proposition 2: The equilibrium point $\boldsymbol{\xi} = \mathbf{0}$ is rendered uniformly globally asymptotically and locally exponentially stable (UGAS/ULES) under assumptions A.1-A.3 when applying (13) with (12) and (33).

Proof: Since the origin of system Σ_2 is UGES (indirectly shown through Proposition 1), the origin of the unperturbed system Σ_1 (i.e., when $\mathbf{z}_{\rm v}^{\rm I} = \mathbf{0}$) is trivially shown to be UGAS/ULES by applying standard Lyapunov theory to (14) and (30), and the interconnection term satisfies $|\mathbf{g}_1(t)| = 1$, the proposed result follows directly from Theorem 7 and Lemma 8 of [18]. ■

Note that the stability property of Proposition 2 is also called global κ-exponential stability, as defined in [20].

3) Step 3: Synchronization Loop Design: In this final design step, we determine the required WMR linear velocity *size* (i.e., $U_{\rm d} = \alpha_{\rm u}$), derived indirectly through $U_{\rm d,m}$, such that a wheeled mobile robot controlled by (13) with (12) and (33) synchronizes with the formation leader. Consequently, consider the positive definite and radially unbounded CLF

$$V_{\tilde{\varpi}} = \frac{1}{2}\tilde{\varpi}^2, \tag{39}$$

where

$$\tilde{\varpi} = \varpi_{\rm c} - \varpi_{\rm l}, \tag{40}$$

and differentiate the CLF with respect to time to get

$$\begin{aligned} \dot{V}_{\tilde{\varpi}} &= \tilde{\varpi}\dot{\tilde{\varpi}} \\ &= \tilde{\varpi}(\dot{\varpi}_{\rm c} - \dot{\varpi}_{\rm l}) \\ &= \tilde{\varpi}(z_{\rm c} + \alpha_{\rm c} - \dot{\varpi}_{\rm l}), \end{aligned}$$

where $z_{\rm c} = \dot{\varpi}_{\rm c} - \alpha_{\rm c}$, and $\alpha_{\rm c}$ represents the desired speed of the collaborator when the mediator has converged to the path, i.e., when $\boldsymbol{\xi} = \mathbf{0}$. Hence, we have that

$$\dot{V}_{\tilde{\varpi}} = \tilde{\varpi}\left(\frac{U_{\rm d,m}}{|\mathbf{p}_{\rm c}'|} - \frac{U_{\rm l}}{|\mathbf{p}_{\rm l}'|}\right) + \tilde{\varpi}z_{\rm c},$$

which is equal to

$$\dot{V}_{\tilde{\varpi}} = -k_{\tilde{\varpi}}\frac{\tilde{\varpi}^2}{\sqrt{\tilde{\varpi}^2+\triangle_{\tilde{\varpi}}^2}} + \tilde{\varpi}z_{\rm c} \tag{41}$$

when choosing

$$U_{\mathrm{d,m}} = |\mathbf{p}_{\mathrm{c}}'| \left(\frac{U_{\mathrm{l}}}{|\mathbf{p}_{\mathrm{l}}'|} - k_{\tilde{\varpi}} \frac{\tilde{\varpi}}{\sqrt{\tilde{\varpi}^2 + \triangle_{\tilde{\varpi}}^2}} \right), \tag{42}$$

where $\triangle_{\tilde{\varpi}} \in [\triangle_{\tilde{\varpi},\,\min}, \infty\rangle$, $\triangle_{\tilde{\varpi},\,\min} > 0$, and where

$$k_{\tilde{\varpi}} = \sigma \frac{U_{\mathrm{l}}}{|\mathbf{p}_{\mathrm{l}}'|},\ \sigma \in \langle 0, 1] \tag{43}$$

ensures that $U_{\mathrm{d,m}}$ satisfies Assumption A.3 by leading to

$$U_{\mathrm{d,m}} = U_{\mathrm{l}} \left(1 - \sigma \frac{\tilde{\varpi}}{\sqrt{\tilde{\varpi}^2 + \triangle_{\tilde{\varpi}}^2}} \right) \frac{|\mathbf{p}_{\mathrm{c}}'|}{|\mathbf{p}_{\mathrm{l}}'|}. \tag{44}$$

Then, expand z_{c} to get

$$\begin{aligned} z_{\mathrm{c}} &= \dot{\varpi}_{\mathrm{c}} - \alpha_{\mathrm{c}} \\ &= \frac{U_{\mathrm{d,m}}(\cos\chi_{\mathrm{r}} - 1) + \gamma s}{|\mathbf{p}_{\mathrm{c}}'|} \end{aligned} \tag{45}$$

where

$$(\cos\chi_{\mathrm{r}} - 1) = \frac{\triangle_{\tilde{\mathrm{e}}} - \sqrt{\tilde{e}^2 + \triangle_{\tilde{\mathrm{e}}}^2}}{\sqrt{\tilde{e}^2 + \triangle_{\tilde{\mathrm{e}}}^2}} \tag{46}$$

such that the system dynamics of $\tilde{\varpi}$ and $\boldsymbol{\xi}$ becomes

$$\Sigma_3 \ : \ \dot{\tilde{\varpi}} = f_3(t, \tilde{\varpi}) + \mathbf{g}_3(t, \boldsymbol{\xi})^{\top} \boldsymbol{\xi} \tag{47}$$

$$\Sigma_4 \ : \ \dot{\boldsymbol{\xi}} = \mathbf{f}_4(t, \boldsymbol{\xi}), \tag{48}$$

which is a cascaded system where the synchronization subsystem is perturbed through the interconnection vector

$$\mathbf{g}_3(t, \boldsymbol{\xi}) = \frac{1}{|\mathbf{p}_{\mathrm{c}}'|} \left[\gamma, U_{\mathrm{d,m}} \frac{\triangle_{\tilde{\mathrm{e}}} - \sqrt{\tilde{e}^2 + \triangle_{\tilde{\mathrm{e}}}^2}}{\tilde{e}\sqrt{\tilde{e}^2 + \triangle_{\tilde{\mathrm{e}}}^2}}, \mathbf{0}_{1\times 2} \right]^{\top}, \tag{49}$$

which is well-defined since

$$\lim_{\tilde{e}\to 0} \frac{\triangle_{\tilde{\mathrm{e}}} - \sqrt{\tilde{e}^2 + \triangle_{\tilde{\mathrm{e}}}^2}}{\tilde{e}\sqrt{\tilde{e}^2 + \triangle_{\tilde{\mathrm{e}}}^2}} = 0. \tag{50}$$

Note that the cascade structure is completely modular in the sense that the control subsystem $(\mathbf{z}_{\mathrm{g}}; \mathbf{z}_{\mathrm{v}}^{\mathrm{I}})$ excites the guidance subsystem $(\tilde{\boldsymbol{\varepsilon}})$, which in turn excites the synchronization subsystem $(\tilde{\varpi})$, see Figure 4.

By considering $\boldsymbol{\zeta} = \left[\tilde{\varpi}, \boldsymbol{\xi}^{\top}\right]^{\top}$, we can now state the following main theorem

Theorem 1: The equilibrium point $\boldsymbol{\zeta} = \mathbf{0}$ is rendered UGAS/ULES under assumptions A.1-A.2 when applying (13) with reference signals (12) and (33) employing (44).

Proof: Since the origin of system Σ_4 is shown to be UGAS/ULES in Proposition 2, the origin of the unperturbed system Σ_3 (i.e., when $\boldsymbol{\xi} = \mathbf{0}$) is trivially shown to be UGAS/ULES by applying standard Lyapunov theory to (39) and (41), and the interconnection term satisfies $|\mathbf{g}_3(t, \boldsymbol{\xi})| < |\mathbf{p}_{\mathrm{p}}'|_{\min}^{-1} \left(\gamma^2 + \left(\frac{U_{\mathrm{l,max}}}{\triangle_{\tilde{\mathrm{e}},\,\min}} \right)^2 \right)^{1/2}$, the proposed result follows directly from Theorem 7 and Lemma 8 of [18]. ■

If every formation member satisfies the conditions of Theorem 1, the formation control problem of (6) is solved.

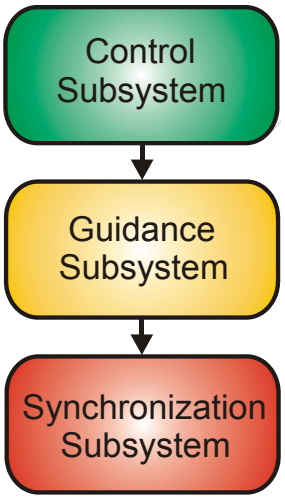

Fig. 4. The modular, cascaded nature of the motion control concept developed for each individual formation member.

III. Discussion

The specific version of the guided scheme that has been treated in this paper is completely decentralized in the sense that no coordination variables are communicated. Hence, the loop is open at the leader-follower level, i.e., the leader propagates without feedback from the followers. Consequently, while impervious to single-point failure, the formation suffers from graceful degradation, i.e., members who cannot keep up with the leader fall out of formation. However, they will still be able to follow their assigned formation positions relative to the path. Thus, this specific scheme could be classified as involving tactical (i.e., local/individual) path following, but strategic (i.e., global/formation-wide) trajectory tracking. An alternative solution involves path following at both the tactical and strategic levels, where the leader receives formation-wide feedback from the followers. Hence, strategic path following values spatial aspects over temporal requirements, while the opposite is true for strategic trajectory tracking. However, this fact does not mean that strategic path following will be preferred for any formation control scenario. For instance, strategic trajectory tracking would typically be chosen for dedicated military operations since such operations usually have tight temporal constraints, and because the scheme inherently involves radio silence.

IV. Case Study: Unicycle-Type WMRs

To illustrate the transient motion behavior associated with the proposed guided formation control scheme, a simulation is carried out in which three unicycle-type WMRs assemble and maintain a given formation along a curved path. Specifically, the desired path is a sinusoid parameterized as $x_{\mathrm{p}}(\varpi) = 10\sin(0.1\varpi)\ [m]$ and $y_{\mathrm{p}}(\varpi) = \varpi\ [m]$; the WMR parameters are $m_{\mathrm{i}} = 5\ [kg]$ and $I_{\mathrm{i}} = 2.5\ [kgm^2]$; the control, guidance, and synchronization parameters are chosen as $k_{\theta,\mathrm{i}} = 1$, $\mathbf{K}_{\nu,\mathrm{i}} = \mathbf{I}$, $\gamma_{\mathrm{i}} = 100$, $\triangle_{\mathrm{e,i}} = \triangle_{\tilde{\varpi},\mathrm{i}} = 1.5$, and $\sigma_{\mathrm{i}} = 0.9$, $\forall i \in \{1, 2, 3\}$; and the speed of the virtual leader is fixed at

$U_1 = 0.25\ [m/s]$. Figure 5 depicts the transient behavior of the formation members as they assemble and maintain a V-shaped formation (defined by $\varepsilon_{\mathrm{f},1} = [-2,-2]^\top$, $\varepsilon_{\mathrm{f},2} = [0,0]^\top$, and $\varepsilon_{\mathrm{f},3} = [-2,2]^\top$) while synchronizing with the virtual leader, as is further illustrated through Figure 6.

V. Conclusions

This paper has addressed the topic of formation control for wheeled mobile robots of the unicycle type. A so-called guided formation control concept was developed within a leader-follower framework by means of a modular design procedure, inspired by integrator backstepping and theory on nonlinear time-varying cascades. The three-step design procedure involved the creation of control, guidance, and synchronization laws for each formation member. These laws ensure that an individual WMR can converge to and maintain its assigned formation position such that the overall formation can assemble and maintain itself while traversing a regularly parameterized path. However, the proposed version of the scheme suffers from graceful degradation due to its completely decentralized nature, which may or may not be a disadvantage. Finally, a computer simulation illustrated the transient motion behavior aspects of the suggested approach.

References

[1] J. P. Desai, J. P. Ostrowski, and V. Kumar, "Modeling and control of formations of nonholonomic mobile robots," *IEEE Transactions on Robotics and Automation*, vol. 17, no. 6, pp. 905–908, 2001.

[2] W. B. Dunbar and R. M. Murray, "Model predictive control of coordinated multi-vehicle formations," in *Proceedings of the 41st IEEE CDC, Las Vegas, Nevada, USA*, 2002.

[3] R. Vidal, O. Shakernia, and S. Sastry, "Formation control of nonholonomic mobile robots with omnidirectional visual servoing and motion segmentation," in *Proceedings of the ICRA'03, Taipei, Taiwan*, 2003.

[4] R. Ghabcheloo, A. Pascoal, C. Silvestre, and I. Kaminer, "Coordinated path following control of multiple wheeled robots with directed communication links," in *Proceedings of the 44th IEEE CDC, Seville, Spain*, 2005.

[5] L. Fang and P. J. Antsaklis, "Decentralized formation tracking of multi-vehicle systems with nonlinear dynamics," in *Proceedings of the MED'06, Ancona, Italy*, 2006.

[6] M. A. Lewis and K.-H. Tan, "High precision formation control of mobile robots using virtual structures," *Autonomous Robots*, vol. 4, pp. 387–403, 1997.

[7] P. Ögren, M. Egerstedt, and X. Hu, "A control lyapunov function approach to multi-agent coordination," in *Proceedings of the 40th IEEE CDC, Orlando, Florida, USA*, 2001.

[8] M. Egerstedt and X. Hu, "Formation constrained multi-agent control," *IEEE Transactions on Robotics and Automation*, vol. 17, no. 6, pp. 947–951, 2001.

[9] M. J. Matarić, "Behaviour-based control: Examples from navigation, learning, and group behaviour," *Journal of Experimental and Theoretical Artificial Intelligence*, vol. 9, pp. 323–336, 1997.

[10] T. Balch and R. C. Arkin, "Behavior-based formation control for multirobot teams," *IEEE Transactions on Robotics and Automation*, vol. 14, no. 6, pp. 926–939, 1998.

[11] J. H. Reif and H. Wang, "Social potential fields: A distributed behavioral control for autonomous robots," *Robotics and Autonomous Systems*, vol. 27, pp. 171–194, 1999.

[12] J. R. T. Lawton, R. W. Beard, and B. J. Young, "A decentralized approach to formation maneuvers," *IEEE Transactions on Robotics and Automation*, vol. 19, no. 6, pp. 933–941, 2003.

[13] G. Antonelli, F. Arrichiello, and S. Chiaverini, "Experiments of formation control with collisions avoidance using the null-space-based behavioral control," in *Proceedings of the MED'06, Ancona, Italy*, 2006.

[14] V. Kumar, N. E. Leonard, and A. S. Morse, Eds., *Cooperative Control*, ser. Lecture Notes in Control and Information Sciences. Springer-Verlag, 2005, vol. 309.

[15] K. Y. Pettersen, J. T. Gravdahl, and H. Nijmeijer, Eds., *Group Coordination and Cooperative Control*, ser. Lecture Notes in Control and Information Sciences. Springer-Verlag, 2006, vol. 336.

[16] G. A. Bekey, *Autonomous Robots: From Biological Inspiration to Implementation and Control*. The MIT Press, Massachusetts, 2005.

[17] M. Krstić, I. Kanellakopoulos, and P. V. Kokotović, *Nonlinear and Adaptive Control Design*. John Wiley & Sons Inc., 1995.

[18] E. Panteley, E. Lefeber, A. Loría, and H. Nijmeijer, "Exponential tracking of a mobile car using a cascaded approach," in *Proceedings of the IFAC Workshop on Motion Control, Grenoble, France*, 1998.

[19] M. Breivik, M. V. Subbotin, and T. I. Fossen, "Guided formation control for fully actuated marine surface craft," in *Proceedings of the 7th IFAC MCMC, Lisbon, Portugal*, 2006.

[20] O. J. Sørdalen and O. Egeland, "Exponential stabilization of nonholonomic chained systems," *IEEE Transactions on Automatic Control*, vol. 40, no. 1, pp. 35–49, 1995.

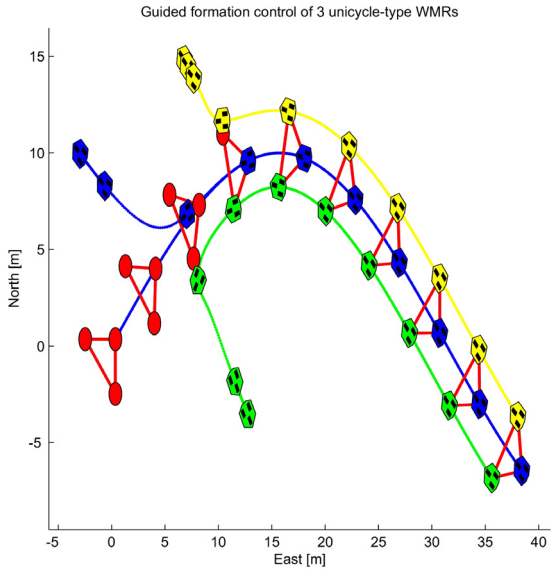

Fig. 5. The transient motion behavior of 3 unicycle-type WMRs assembling and maintaining a V-shaped formation that traverses a sinusoidal path.

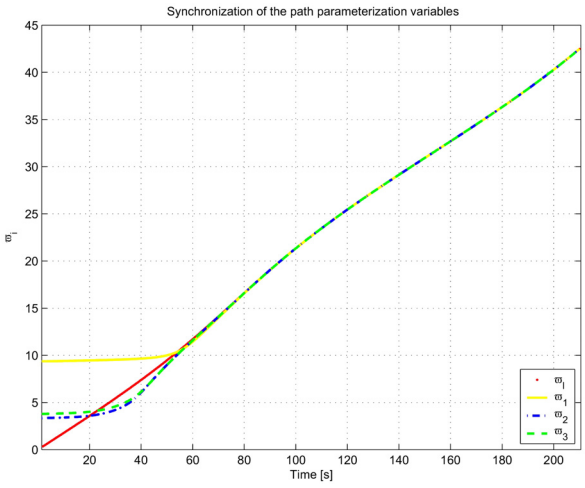

Fig. 6. The involved path parameters synchronize as intended.